International Journal of Control

ISSN: 0020-7179 (Print) 1366-5820 (Online) Journal homepage: https://www.tandfonline.com/loi/tcon20

A sliding mode estimation method for fluid flow fields using a differential inclusions-based analysis

Krishna Bhavithavya Kidambi, William MacKunis, Sergey V. Drakunov & Vladimir Golubev

To cite this article: Krishna Bhavithavya Kidambi, William MacKunis, Sergey V. Drakunov & Vladimir Golubev (2020): A sliding mode estimation method for fluid flow fields using a differential inclusions-based analysis, International Journal of Control, DOI: 10.1080/00207179.2020.1713403

To link to this article: https://doi.org/10.1080/00207179.2020.1713403

Accepted author version posted online: 08 Jan 2020.
Published online: 22 Jan 2020.

INTERNATIONAL JOURNAL OF CONTROL
https://doi.org/10.1080/00207179.2020.1713403

Taylor & Francis
Taylor & Francis Group

A sliding mode estimation method for fluid flow fields using a differential inclusions-based analysis

Krishna Bhavithavya Kidambi [a], William MacKunis[b], Sergey V. Drakunov[b] and Vladimir Golubev[c]

[a]Institute for Systems Research, University of Maryland, College Park, MD, USA; [b]Department of Physical Sciences, Embry-Riddle Aeronautical University, Daytona Beach, FL, USA; [c]Department of Aerospace Engineering, Embry-Riddle Aeronautical University, Daytona Beach, FL, USA

ABSTRACT

A sliding mode observer (SMO) design and convergence analysis are presented in this paper, which includes a rigorous treatment to address multiple discontinuities in the resulting estimation error dynamics. In an extension of our previous SMO results, the current work provides a non-trivial reworking of the SMO estimation error system development and stability analysis that incorporates differential inclusions. The specific contributions presented in this paper beyond the previous work include: **(1)** A differential inclusions-based analysis of the SMO, which incorporates the set-valued definition of the discontinuous signum function; **(2)** An expanded derivation of the estimation error dynamics, which emphasises advantageous properties particular to our SMO structure; **(3)** A Lyapunov-based stability analysis of the SMO, that rigorously incorporates the multiple discontinuities in the estimation error dynamics. The Lyapunov-based stability analysis proves that the SMO achieves finite-time estimation of the complete state vector, where the output equation is in a nonstandard mathematical form. To test the performance of the SMO, numerical simulation results are also provided, which demonstrate the capability of the SMO to estimate the state of a fluid flow dynamic system using only a single sensor measurement of the flow field velocity.

ARTICLE HISTORY
Received 13 July 2019
Accepted 28 December 2019

KEYWORDS
Sliding mode observer; differential inclusion; nonlinear estimation; control applications; Lyapunov

1. Introduction

Practical implementation of feedback control systems can be significantly hindered by sensor limitations, unmeasurable states, and sensor measurement noise and delays. Motivated by these challenges, the design of observers (or estimators) is an essential component in most control engineering applications to provide the state measurements required to design stabilising feedback control laws. In light of this, plethora of research has been done focusing on developing sliding mode observers to generate state estimates for various classes of systems (Drakunov & Utkin, 1992; Shtessel, Edwards, Fridman, & Levant, 2014; Utkin, 1978, 2013). But, SMO often utilise high-bandwidth switching strategies to estimate the complete state of a dynamic system using only the available sensor measurements. In light of this several new SMO methods have been shown to achieve superior state estimation performance through the use of strategies such as twisting, super-twisting, and higher-order SMO techniques (e.g. see Floquet & Barbot, 2006, 2007; Fridman, Shtessel, Edwards, & Yan, 2008; Levant, 2003). The motivation of the current paper is to address the specific challenges that can arise in practical control applications where the resulting dynamic equations contain discontinuities resulting from the use of the signum function as in standard SMO methods and provide rigorous stability analysis for such class of systems. To cope with the discontinuities and uncertainties that can arise in the mathematical models of SMO estimation error dynamics, differential inclusions provide a important mathematical tool that can be applied to rigorously analyse the convergence performance of SMO. The differential inclusions present a natural step in generalising study of systems where discontinuities occur in the model or being introduced for control and estimation purposes. They allow expanding the class of systems under consideration and address uncertainties in their behaviour.

Differential inclusions have gained significant interest in providing stability analyses for nonsmooth systems (Clarke, Ledyaev, & Stern, 1998; Doris et al., 2008; Filippov, 2013; Liu, Sun, Liu, & Teel, 2016; Sadikhov & Haddad, 2015; Vijayakumar, 2018). The fundamental properties and solutions of discontinuous systems are discussed in Filippov (2013). In Clarke et al. (1998) the existence of smooth Lyapunov functions for stable differential inclusions is discussed. In Sadikhov and Haddad (2015), a feedback control law for discontinuous systems is designed based on the existence of a nonsmooth Lyapunov function. An invariance theorem for nonautonomous delay differential inclusions is provided in Liu et al. (2016), for the case where the candidate functional is bounded by a continuous negative semi-definite function. Recently Vijayakumar (2018), provided sufficient conditions for approximate controlability for a nonlinear resolvent integro-differential inclusions in Hilbert space.

Many researchers have paved the path for analysing the theory of differential inclusions for various engineering applications: Robotics – (Paden & Sastry, 1987); Hybrid systems – (Goebel, Sanfelice, & Teel, 2009); Under water Vehicle – (Fischer, Hughes, Walters, Schwartz, & Dixon, 2014); Switched

CONTACT William MacKunis mackuniw@erau.edu

nonlinear systems - (Teel, Nešić, Lee, & Tan, 2016); Neural networks – (Matusik, Nowakowski, Plaskacz, & Rogowski, 2018; Shi et al., 2019; Wang, Shi, Huang, Zhong, & Zhang, 2018); Chua circuits (Shi et al., 2018). While the theory of differential inclusions has been widely investigated to analyse the behaviour of discontinuous systems, there remains a need for new theoretical tools to rigorously analyse the performance of discontinuous SMO.

The design and analysis of control systems and observers for multi-valued or discontinuous systems has been addressed by several recent research results (Brogliato & Heemels, 2009; Fischer, Kamalapurkar, & Dixon, 2013; Osorio & Moreno, 2006; Tanwani, Brogliato, & Prieur, 2014). In Osorio and Moreno (2006), an observer method is presented for a class of discontinuous systems based on the dissipativity method, with a linear time-invariant system in the feedforward path and a discontinuous nonlinear system in the feedback path. The observer design in Tanwani et al. (2014), Brogliato and Heemels (2009) covers systems in Lur'e form, with multivalued nonlinearities using a high gain approach and with multivalued mappings in the feedback path respectively. Two generalised corollaries to the Lasalle–Yoshizawa theorem are presented in Fischer et al. (2013) to address systems with discontinuous right hand sides. The corollaries in Fischer et al. (2013) are used to develop a rigorous analysis of a robust and adaptive nonlinear control method that has a discontinuity in the closed-loop error dynamics. The aforementioned research results have provided much insight into analysing the behaviour of estimation and control systems with discontinuities. The focus of this paper is on differential inclusions-based stability analysis of a hierarchical SMO strategy for which the resulting estimation error dynamics contain multiple discontinuities.

A hierarchical SMO design and convergence analysis are presented in this paper, which includes a rigorous treatment to address multiple right-hand side (RHS) discontinuities in the estimation error dynamics. By leveraging our previous SMO results in Drakunov (1992), Kidambi, Ramos-Pedroza, MacKunis, and Drakunov (2016), Kidambi, MacKunis, Ramos-Pedroza, and Drakunov (2017), the current work provides a non-trivial reworking of the error system development and stability analysis using a Filippov solution. The specific contributions presented in this paper beyond the previous work include:

- A differential inclusions-based analysis of the SMO, which utilises the set-valued definition of the discontinuous signum function;
- An expanded derivation of the estimation error dynamics, which emphasises advantageous properties particular to our SMO structure;
- A Lyapunov-based stability analysis of the SMO, that rigorously addresses the multiple discontinuities in the estimation error dynamics.

To test the performance of the SMO, numerical simulation results are also provided, which demonstrate the capability of the SMO to estimate the state of a fluid flow dynamic system using only a single sensor measurement of the flow field velocity.

2. Preliminaries

In this section, we provide background on the mathematical tools utilised to address the challenges involved in analysing the behaviour of differential equations with discontinuous RHS. While the generalised solutions of differential equations with continuous RHS are well known, the presence of discontinuities necessitates modified mathematical approaches to obtain the solutions. In this paper, we utilise *differential inclusions* to handle the challenge of analysing the stability of a SMO method, where the equations of the error dynamics contain discontinuities.

2.1 Mathematical definitions

Consider a nonlinear system defined as

$$\dot{x} = f(x,t), \tag{1}$$

where $x(t) \in \mathcal{X} \subset \mathbb{R}^n$ denotes the state vector, $f : \mathcal{X} \times [0,\infty) \to \mathbb{R}^n$ is Lebesgue measurable and essentially locally bounded, uniformly in t; and $\mathcal{X}$ is an open and connected set. The definition of a solution to (1) is well established for the case where f is Lipschitz continuous; however, this basic definition is not applicable if there exists a discontinuity in f at any point in $\mathcal{X}$. To address the case where f contains discontinuities, differential inclusions can be utilised to obtain the generalised solution of (1) at a point of discontinuity by analysing the behaviour of the derivative of f at neighbouring points (Filippov, 1988; Krasovskii, 1963).

Remark 2.1 (Stability of Systems with Discontinuous RHS)**:** The stability of closed-loop systems in the form of (1) with continuous right-hand sides can be analysed using existing Lyapunov theory (Khalil, 1996; Slotine & Li, 1991). However, these theorems must be modified to analyse systems with discontinuous RHS (Fischer et al., 2013; Guo & Huang, 2009). The differences between Lyapunov analyses for systems with continuous and discontinuous systems include: differential equations are replaced with differential inclusions, points are replaced with sets, and gradients are replaced by generalised gradients.

The following definitions are provided to facilitate the subsequent analysis.

Definition 2.1 (Filippov Solution Filippov, 1988; Shevitz & Paden, 1994)**:** A function $x(t)$ is called a solution to (1) on the interval $[0,\infty)$ if $x(t)$ is absolutely continuous and for almost all $t \in [0,\infty)$

$$\dot{x} = K[f](x(t),t), \tag{2}$$

where $K[f](x(t),t)$ denotes an upper semi-continuous, non empty, compact and convex valued map on $\mathcal{X}$, defined as

$$K[f](x(t),t) \triangleq \bigcap_{\epsilon>0} \bigcap_{\mu N=0} \overline{co} f(B(x(t),\epsilon) - N, t), \tag{3}$$

where $\bigcap_{\mu N=0}$ denotes the intersection over sets N of Lebesgue measure zero, and $\overline{co}$ denotes convex closure. In (3), $B(x(t),\epsilon)$ is the open set defined as

$$B(x(t),\epsilon) \triangleq \left\{ v \in \mathbb{R}^n \,|\, \|x(t) - v\| < \epsilon \right\}. \tag{4}$$

A simple example to illustrate the definitions in (2)–(4) is provided in the subsequent Section 2.2.

Definition 2.2 (Directional Derivative Kaplan, 1991)**:** The right directional derivative of a function $f : R^m \to R^n$, at $x \in \mathbb{R}^m$ in the direction of $v \in R^m$ is defined as

$$f'(x,v) = \lim_{t\to 0^+} \frac{f(x+tv) - f(x)}{t}. \tag{5}$$

The generalised directional derivative of f at x in the direction of v is defined as

$$f^0(x,v) = \lim_{y\to x} \sup_{t\to 0^+} \frac{f(y+tv) - f(y)}{t}. \tag{6}$$

Definition 2.3 (Regular Function Clarke, 1983)**:** A function $f : R^m \to R^n$ is regular at $x \in R^m$, if the right directional derivative of f at x in the direction of v exists $\forall v \in R^m$, and $f'(x,v) = f^0(x,v)$.

Definition 2.4 (Clarke's Generalized Gradient Clarke, 1983)**:** Given a function $V : \mathbb{R}^n \times [0,\infty) \to \mathbb{R}$, where $V(x,t)$ is locally Lipschitz in (x,t), the generalised gradient of V at (x,t) is defined as

$$\partial V(x,t) = \overline{co}\left\{\lim \nabla V(x_i,t_i) \middle| (x_i,t_i) \to (x,t), (x_i,t_i) \notin \Omega_V\right\}, \tag{7}$$

where Ω_V denotes the set of measure zero where the gradient of V is not defined [Rademacher's theorem-(Nekvinda & Zajíček, 1988)].

Lemma 2.1 (Chain Rule Paden & Sastry, 1987; Shevitz & Paden, 1994)**:** *Let $V : \mathbb{R}^n \times [0,\infty) \to \mathbb{R}$ be a regular, Lipschitz function. If $x(t)$ a Filippov solution of $\dot{x} = f(x,t)$, then $\frac{\mathrm{d}}{\mathrm{d}t}V(x(t),t)$ exists almost everywhere (a.e.) for $t \geq 0$, and $\dot{V}(x(t),t) \overset{a.e.}{\in} \dot{\tilde{V}}(x(t),t)$ where*

$$\dot{\tilde{V}}(x(t),t) \triangleq \bigcap_{\xi \in \partial V(x(t),t)} \xi^T \begin{bmatrix} K[f](x(t),t) \\ 1 \end{bmatrix}. \tag{8}$$

Proof of Lemma 2.1 *can be found in Shevitz and Paden (1994) and Paden and Sastry (1987) and is omitted for brevity.*

2.2 Simple example of differential inclusion

The concept of Filippov's solution is illustrated using a simple scalar differential equation (Paden & Sastry, 1987)

$$\dot{x} = -\mathrm{sgn}(x); \quad x(0) = 1. \tag{9}$$

The state is 1 at time 0 and moves at constant velocity -1 until it reaches 0 and remains at the point of discontinuity in the right hand side of (9). In fact, this is Filippov's solution to (9). Since $B(0,\epsilon), \epsilon > 0$, an open interval containing the origin, intersects both $(-\infty, 0)$ and $(0,\infty)$ on the sets of positive measure, we have that $K[-sgn](0) = \overline{co}\{-1,1\} = [-1,1]$. For general x, the differential inclusion (2) and (4) becomes

$$\dot{x} \in -\mathrm{SGN}(x), \tag{10}$$

where SGN is the set-valued sign function defined as Paden and Sastry (1987)

$$\mathrm{SGN}(x) \triangleq \begin{cases} \{1\} & \text{if } x > 0 \\ [-1,1] & \text{if } x = 0 \\ \{-1\} & \text{if } x < 0 \end{cases}. \tag{11}$$

3. Observer design

This section presents a SMO design for a class of autonomous, nonlinear systems. Specifically, a rigorous analysis is utilised to derive a set of estimation error dynamic equations, the right-hand side of which contains discontinuities resulting from the use of the sgn$(\cdot)$ function in the SMO equation. A detailed analysis is also provided to define the sets within which discontinuities exist.

3.1 Dynamic model and properties

Consider a class of nonlinear systems given by

$$\dot{x} = f(x), \tag{12}$$

$$y = h(x), \tag{13}$$

where $x : [0,\infty) \to \mathbb{R}^n$ denotes the state vector, and $y : \mathbb{R}^n \to \mathbb{R}$ is the system output (e.g. sensor measurement). In (12) and (13), $f : \mathbb{R}^n \to \mathbb{R}^n$ and $h : \mathbb{R}^n \to \mathbb{R}$ are sufficiently smooth vector functions as described in the subsequent Assumption 3.1.

To facilitate the subsequent observer design and convergence analysis, an auxiliary measurement vector $H : \mathbb{R}^n \to \mathbb{R}^n$ is defined as Drakunov (1992), Kidambi et al. (2016), Kidambi et al. (2017), Kidambi, Ramos-Pedroza, MacKunis, and Drakunov (2019)

$$H(x) \triangleq \begin{bmatrix} h_1(x) & \cdots & h_n(x) \end{bmatrix}^T, \tag{14}$$

where

$$h_1(x) = h(x), \tag{15}$$

$$h_{i+1}(x) = \frac{\partial h_i(x)}{\partial x} f(x). \tag{16}$$

The function $h_{i+1}(x)$ is the i^{th} Lie (directional) derivative of $h(x)$ along the trajectories of the system described in (12). Thus, the elements of $H(x)$ can be expressed as

$$h_i(x) = L_f^{i-1} h(x). \tag{17}$$

Based on (12) and (15) it follows that, if x is a solution of (12), then

$$\frac{\mathrm{d}}{\mathrm{d}t} h_i(x) = h_{i+1}(x). \tag{18}$$

Assumption 3.1: If $x(t) \in \mathcal{L}_\infty$, the first $n-1$ partial derivatives of $f(x)$ and first n partial derivatives of $h(x)$ exist and are bounded in the sense that $\frac{\partial^{n-1} f(x)}{\partial x^{n-1}} \in \mathcal{L}_\infty$ and $\frac{\partial^n h(x)}{\partial x^n} \in \mathcal{L}_\infty$.

The differentiabilty requirements described in Assumption 1 stem from the use of repeated Lie derivatives in the observer structure as defined explicitly in Equations (15)–(18), along with the subsequent bounding conditions in Inequality (33). Although Assumption 1 is fairly restrictive, our subsequent Simulation Results section presents an example of a practical system (i.e. reduced-order fluid flow dynamic model) which satisfies Assumption 1. Future work will investigate extensions of the current observer design, in which Assumption 1 can be relaxed or eliminated.

Assumption 3.2: For a given domain $\mathcal{X}_0 \subset \mathbb{R}^n$ of initial conditions of the system (12), all solutions of (12) belong to the open one-component domain $\mathcal{X} \subset \mathbb{R}^n$, for all $t \in [0, \infty)$.

Condition 3.1 (Observability)**:** The Jacobian $\mathcal{O} \triangleq \frac{\partial H(x)}{\partial x}$ of the continuous map $H(x)$ is nondegenerating in $\mathcal{X}$ in the sense that

$$|\det \mathcal{O}| \geq \delta > 0$$

for some δ and for every $x \in \mathcal{X}$.

From Condition 3.1, the Jacobian matrix $\mathcal{O}$ is invertible. This fact will be utilised in the subsequent SMO design.

3.2 Observer design

Under Condition 3.1, an observer that estimates the full state x of the system in (12) using only output measurements y can be designed as

$$\dot{\hat{x}} = f(\hat{x}) + \mathcal{O}^{-1}(\hat{x})\, M(\hat{x})\, \text{sgn}\left(\Phi(t) - H(\hat{x})\right), \tag{19}$$

where $\mathcal{O}(\cdot)$ is introduced in Condition 3.1, and $\hat{x} : [0, \infty) \to \mathbb{R}^n$ denotes the estimate of the state x in (12). In (19) $\text{sgn}(\cdot)$ operates element-wise on the vector argument so that $\text{sgn}(\zeta) \triangleq [\text{sgn}(\zeta_1)\ \text{sgn}(\zeta_2)\ \cdots\ \text{sgn}(\zeta_n)]^T\ \forall \zeta \in \mathbb{R}^n$. Also in (19), $M : \mathbb{R}^n \to \mathbb{R}^{n \times n}$ denotes a diagonal matrix with positive elements defined as

$$M(\hat{x}) = \text{diag}\left(m_1(\hat{x}), \ldots, m_n(\hat{x})\right), \tag{20}$$

where $m_i : \mathbb{R}^n \to \mathbb{R}^+$, for $i = 1, \ldots, n$, denote control gains, which could be constant or could depend on $\hat{x}$ in general. In (19), $\Phi : [0, \infty) \to \mathbb{R}^n$ is defined as

$$\Phi(t) = [\phi_1(t), \ldots, \phi_n(t)]^T, \tag{21}$$

where the elements $\phi_i(t)$ are defined via the recursive relationship

$$\phi_1(t) = y(t) \tag{22}$$

$$\phi_{i+1}(t) = m_i(\hat{x})\text{sgn}\left(\phi_i(t) - h_i(\hat{x})\right) \tag{23}$$

for $i = 1, \ldots, n-1$.

Remark 3.1 (Measurable Auxiliary Signals)**:** Based on (22), $\phi_1(t)$ is simply the measurable output of the system in (12) and (13). Further, the recursion relation in (23) ensures that the auxiliary signals $\phi_2(t), \phi_3(t), \cdots, \phi_n(t)$ are also measurable throughout observer operation. Indeed, it follows from (23) that the auxiliary signals depend only on $y(t)$ and $\hat{x}(t)$.

Through judicious design of the gain matrix M, it can be shown that the observer in (19) estimates the state $x(t)$ in a finite time interval. The choice of M is based on the region $\mathcal{X}_0$ of initial conditions for the system (12) and on the upper bounds of $h_i(x)$. This proof is provided via Lyapunov-based stability analysis in the subsequent Section 5.

4. SMO estimation error dynamics

4.1 Objective

Under Condition 3.1, the map H in (14) is a diffeomorphism (i.e. there is a one-to-one correspondence between x and H). Since H is a diffeomorphism, it follows that $H(x) - H(\hat{x}) \to 0 \Rightarrow x - \hat{x} \to 0$. Thus, to quantify the estimation objective, it is sufficient to define the estimation error as

$$e(t) = H(x) - H(\hat{x}), \tag{24}$$

where $e(t) \triangleq [e_1(t)\ \cdots\ e_n(t)]^T$ represents the estimation error. The estimation objective can therefore be mathematically stated as

$$\|e(t)\| \to 0, \tag{25}$$

where $\|\cdot\|$ in (25) denotes the standard Euclidean norm (or 2-norm). Note that the choice to use the 2-norm is arbitrary, and the subsequent stability analysis could be used to prove convergence of the observer error using the p-norm definition in general.

4.2 Estimation error dynamics

The estimation error dynamics can be obtained by taking the time derivative of (24) as

$$\dot{e}(t) = \frac{\partial H(x)}{\partial x}\dot{x} - \frac{\partial H(\hat{x})}{\partial x}\dot{\hat{x}}. \tag{26}$$

After using (1) and (19), the estimation error dynamics can be expressed as

$$\dot{e}(t) = \frac{\partial H(x)}{\partial x} f(x) - \frac{\partial H(\hat{x})}{\partial x} f(\hat{x}) - M(\hat{x})\, sgn\left(\Phi(t) - H(\hat{x})\right), \tag{27}$$

where the fact that $\mathcal{O}(\hat{x}) = \frac{\partial H(x)}{\partial x}|_{x=\hat{x}}$ was utilised.

Remark 4.1: Note that the estimation error dynamic equation in (27) is in the form of (1), where the RHS includes discontinuities resulting from the use of the sliding mode observer introduced in (19). The use of differential inclusions provides for existence of solutions, and the subsequent estimator convergence analysis will be provided utilising the definition of the Filippov solution presented in Section 2.

To facilitate the subsequent Lyapunov-based stability analysis, the definitions in (15) and (16) will be used to rewrite the

error dynamics in (27) as

$$\begin{bmatrix} \dot{e}_1(t) \\ \dot{e}_2(t) \\ \vdots \\ \dot{e}_n(t) \end{bmatrix} = \begin{bmatrix} h_2(x) - h_2(\hat{x}) \\ h_3(x) - h_3(\hat{x}) \\ \vdots \\ h_{n+1}(x) - h_{n+1}(\hat{x}) \end{bmatrix} - \begin{bmatrix} m_1(\hat{x})\,\mathrm{sgn}(\sigma_1) \\ m_2(\hat{x})\,\mathrm{sgn}(\sigma_2) \\ \vdots \\ m_n(\hat{x})\,\mathrm{sgn}(\sigma_n) \end{bmatrix} \tag{28}$$

where $\sigma_i : \mathbb{R}^n \to \mathbb{R}$ denote sliding surfaces for the i^{th} estimation error that are defined explicitly as

$$\sigma_i \triangleq \phi_i(t) - h_i(\hat{x}) \tag{29}$$

for $i = 1, \ldots, n$, where $\phi_i(t)$ are defined in (22) and (23). The estimation error dynamic equations in (28) can be rewritten in the compact form

$$\dot{e}_i(t) = h_{i+1}(x) - h_{i+1}(\hat{x}) - m_i(\hat{x})\, sgn(\sigma_i) \tag{30}$$

for $i = 1, \ldots, n$.

Property 1 (Sliding Surface Definition)**:** Based on the definitions in (13), (15), (22) and (29), it follows by definition that

$$\sigma_1(t) = e_1(t). \tag{31}$$

Property 1 will be utilised in the subsequent convergence analysis of the proposed SMO.

4.3 Hierarchical analysis of estimation error dynamics

The motivation for expressing the estimation error dynamics in the forms given in (28) and (30) is based on the recursive structure of the auxiliary signals in (22) and (23). The decoupling between the individual elements of the estimation error dynamics for $e_i(t)$, for $i = 1, \ldots, n$, is highlighted in (30) to facilitate the hierarchical strategy of the convergence analysis in the subsequent Stability Analysis Section.

Theorem 4.1 (Sliding Surface Convergence)**:** *The hierarchical definition of the auxiliary signals $\phi_i(t)$, for $i = 1, \ldots, n$, in* (22) *and* (23) *can be used along with* (29) *and* (30) *to show that*

$$e_i(t) = 0 \Rightarrow \sigma_{i+1}(t) = e_{i+1}(t) \tag{32}$$

for $i = 1, \ldots, n$, provided the observer gains $m_i(\hat{x})$, for $i = 1, \ldots, n$, are selected to satisfy the sufficient condition

$$m_i(\hat{x}) > \left| h_{i+1}(x) - h_{i+1}(\hat{x}) \right|. \tag{33}$$

Proof: By using (30), the following can be obtained immediately:

$$e_i(t) = 0 \Rightarrow \dot{e}_i(t) = 0 \Rightarrow \tag{34}$$

$$h_{i+1}(x) = m_i(\hat{x})\mathrm{sgn}(\sigma_i). \tag{35}$$

Based on the recursive definition of $\phi_i(t)$ in (23), it follows from (35) that $\phi_{i+1}(t) = h_{i+1}(x)$. Thus, $\sigma_{i+1}(t) = h_{i+1}(x) - h_{i+1}(\hat{x})$ from (29). Hence, (32) can be obtained from (24). This proves Theorem 4.1. ■

5. Stability analysis

Theorem 5.1 (Observer Convergence)**:** *For the class of nonlinear systems described by Equations* (12) *and* (13)*, the observer described in* (14), (19)–(21) *ensures that all system states and estimates remain bounded and that finite-time estimation of the complete system state x(t) is achieved in the sense that*

$$\|e(t)\| \equiv 0 \quad \text{for } t \geq t_n < \infty \tag{36}$$

using only measurements y(t), provided the observer gains m_i, for $i = 1, ldots, n$, are selected to satisfy Inequality (33)*, and where $t_n \in \mathcal{L}_\infty$ are (finite) calculable time instants that are explicitly derived in the appendix.*

Proof: Let $V_i : \mathbb{R} \times [0, \infty) \to \mathbb{R}$, for $i = 1, \ldots, n$, be locally Lipschitz, positive definite, Lyapunov candidate functions defined as

$$V_i = \frac{1}{2} e_i^2. \tag{37}$$

After taking the time derivative of (37), $\dot{V}_i(e_i) \overset{a.e.}{\in} \dot{\tilde{V}}_i(e_i)$ and

$$\dot{\tilde{V}}_i(e_i, t) \triangleq \underset{\xi_i \in \partial V_i(e_i,t)}{\cap} \xi_i^T K \begin{bmatrix} \dot{e}_i \\ 1 \end{bmatrix}(e_i, t). \tag{38}$$

Given that the Lyapunov candidate function in (37) is continuously differentiable, the generalised gradient reduces to the standard gradient (Fischer et al., 2013), and thus, (38) can be expressed as

$$\dot{\tilde{V}}_i \subset \nabla_i V_i^T K[\dot{e}_i](e_i) \subset e_i^T K[\dot{e}_i], \tag{39}$$

where $\nabla_i \triangleq \partial / \partial e_i$, for $i = 1, \ldots, n$. By using (30), the equation in (39) can be rewritten as

$$\dot{\tilde{V}}_i \subset e_i^T \left(h_{i+1}(x) - m_i(\hat{x}) K \left[\mathrm{sgn}(\sigma_i(t)) \right] \right) \tag{40}$$

for $i = 1, \ldots, n$, where $K[\mathrm{sgn}(\cdot)] = \mathrm{SGN}(\cdot)$ denotes the set-valued signum function defined in (11).

To complete the stability proof, *Property 1 and Theorem 1* will be leveraged, and the proof will be carried out sequentially. To this end, consider the case where $i = 1$, for which the expression in (40) becomes

$$\dot{\tilde{V}}_1 \subset e_1^T \left(h_2(x) - m_1(\hat{x})\, \mathrm{SGN}(e_1) \right), \tag{41}$$

where the definition in (31) of Property 1 was utilised. The scalar inequality in (41) can be reduced and upper bounded as

$$\dot{\tilde{V}}_1 \leq - \left(m_1(\hat{x}) - |h_2(x)| \right) |e_1|. \tag{42}$$

The reduction of the set in (41) to the scalar inequality in (42) results from the fact that the set-defined term $K[sgn(e_1)]$ is

multiplied by e_1. Thus, when $e_1 = 0$, it follows that

$$(0)\ \text{SGN}\,(0) = \{0\}\,. \tag{43}$$

By selecting the gain $m_1(\hat{x})$ according to the sufficient condition in (33), the upper bound in (42) can be expressed as

$$\dot{\tilde{V}}_1 \leq -\kappa_1 \left|e_1\right| \tag{44}$$

where $\kappa_1 \in \mathbb{R}^+$ is a known bounding constant. Inequality (44) can now be used along with (37) to prove finite-time convergence of $e_1(t)$ in the sense that

$$|e_1| \equiv 0, \quad \text{for } t \geq t_1,$$

where $t_1 \in \mathcal{L}_\infty$ can be computed.

Given that $e_1(t) \equiv 0$ for $t \geq t_1$, (32) of Property 2 can be used to show that $\sigma_2(t) = e_2(t)$, and thus, the set (40) for $i = 2$ can be expressed as

$$\dot{\tilde{V}}_2 \subset e_2^T \left(h_3(x) - m_2(\hat{x})\text{SGN}\,(e_2)\right). \tag{45}$$

The scalar inequality in (45) then reduces to

$$\dot{\tilde{V}}_2 \leq -\left(m_2\left(\hat{x}\right) - \left|h_3\left(x\right)\right|\right)\left|e_2\right|. \tag{46}$$

By again using the sufficient gain condition in (33), (46) can be expressed as

$$\dot{\tilde{V}}_2 \leq -\kappa_2 \left|e_2\right| \tag{47}$$

where $\kappa_2 \in \mathbb{R}^+$ is a known bounding constant. The inequality in (47) can be used along with (37) (for $i = 2$) to prove that

$$|e_2| \equiv 0, \quad \text{for } t \geq t_2,$$

where $t_2 \in \mathcal{L}_\infty$ is calculable. Continuing in this sequential manner, and leveraging Theorem 4.1, it follows that

$$|e_i| \equiv 0, \quad \text{for } t \geq t_i$$

for $i = 3, \ldots, n$, provided the sufficient condition in (33) is satisfied. Thus, the objective in (36) of Theorem 5.1 is proved. ■

Remark 5.1 (Implementation of the SMO)**:** It should be noted that, although the convergence proof of the proposed SMO was provided in a sequential manner, the SMO implementation does not require any special treatment. The sequential analysis used for the proof in this section was provided for clarity of the presentation only. Indeed, the simulation results in the following section were obtained by implementing the estimator with a single fixed set of observer gains m_i, for $i = 1, \ldots, n$, which was selected a single time at observer initialisation.

6. Simulation study: flow field velocity estimation

A numerical simulation was created to test the performance of the proposed SMO. The simulation is based on the observer design described in (19)–(23). The simulation tests the capability of the proposed SMO to estimate the complete state of a fluid flow dynamic system using only sensor measurements of the flow field velocity.

6.1 Reduced-order model derivation

A challenge in designing an observer for such systems is that fluid flow dynamics are governed by complex models such as the Burgers' equations or Navier–Stokes equations, which are partial differential equations (PDEs). In this example, we will consider the Navier–Stokes equations, which can be expressed as

$$\nabla \cdot \upsilon = 0, \quad \frac{\partial \upsilon}{\partial t} = -(\upsilon \cdot \nabla)\upsilon + \frac{1}{Re}\nabla^2(\upsilon) - \nabla p, \tag{48}$$

where $\upsilon(s,t) : \Omega \times [0,\infty) \in \mathbb{R}^3$ denotes the velocity of the flow field over a spatial domain $s \in \Omega \subset \mathbb{R}^3$, where $\frac{1}{Re}$ is kinematic viscosity.

Proper orthogonal decomposition (POD)-based model order reduction is utilised to recast the PDE dynamic model into a finite set of ordinary differential equations (ODEs). In the POD modal decomposition technique, the flow field velocity $\upsilon(s,t)$ is expanded as a weighted sum of POD modes defined in the spatial domain Ω as

$$\upsilon(s,t) = \upsilon_0 + \sum_{i=1}^{n} x_i(t)\psi_i(s). \tag{49}$$

In (49), $\psi_i(s) \in \mathbb{R}^3$, denote the POD modes and $x_i(t)$, $i = 1, \ldots, n$, denote unknown, time-varying coefficients resulting from the modal decomposition. By substituting the velocity field expansion (49) into (48), the POD-based reduced-order model of the Navier–Stokes equations is obtained as

$$\dot{x}_k(t) = L_k x(t) + x^T(t) Q_k x(t) + b_k, \quad k = 1, \ldots, n \tag{50}$$

$L_k(s) \in \mathbb{R}^{1\times n}$, $Q_k(s) \in \mathbb{R}^{n\times n}$, and $b_k \in \mathbb{R}$, denote constant parameter matrices, which can be explicitly obtained from a given set of experimental or high-fidelity simulation data. The expression in (50) represents a system of nonlinear ordinary differential equations resulting from POD-based model order reduction. The system of ODEs in (50) can be expressed in the general form given in (12). For additional details on POD-based model order reduction, readers are referred to Holmes, Lumley, and Berkooz (1996), Chatterjee (2000), MacKunis, Drakunov, Reyhanoglu, and Ukeiley (2011). Further details on the POD-based modal decomposition from (48) → (50) can be found in Kidambi et al. (2019), MacKunis et al. (2011). The reduced-order model resulting from POD contains an unmeasurable state vector containing the time-varying coefficients from Galerkin projection.

The flow field observer design presented here is based on the standard assumption that one or more sensor measurements are available. By using the similar POD modal decomposition analysis the output measurement equation can be expressed as Holmes et al. (1996), Chatterjee (2000)

$$y(t) = Cx(t), \tag{51}$$

where $y(t) \in \mathbb{R}$, and $C \in \mathbb{R}^{1\times n}$ is a vector of known constants, and $x(t) = [x_1(t), x_2(t), \ldots, x_n(t)]^T$ is introduced in (50). Physically, the expression in (51) can be interpreted as the measured velocity at a predefined location as approximated in terms of the POD modes. Specifically, the plant model in (50) and the output equation in (51) can be expressed in the form given in (12) and (13).

Table 1. Parameters used in the simulation plant model (Gordeyev & Thomas, 2013).

Linear terms		Quadratic and cubic terms	
$b_1 = 557.7$	$L_{11} = -86.1$	$Q_{111} = 1.8$	$Q_{414} = 2.9$
$b_2 = 1016.9$	$L_{22} = -392.4$	$Q_{121} = -2.2$	$Q_{424} = -9.8$
$b_3 = 41.0$	$L_{23} = 263.9$	$Q_{131} = -2.3$	$Q_{434} = 6.3$
$b_4 = -628.9$	$L_{32} = -218.3$	$Q_{141} = -6.8$	$Q_{444} = -7.3$
	$L_{33} = -7.6$	$Q_{212} = 75.0$	
	$L_{41} = 43.4$	$Q_{313} = 5.0$	$t_2 = -2.5$
	$L_{44} = -113.5$	$Q_{314} = 3.9$	$t_3 = -0.2$

6.2 Simulation results

The flow field dynamic reduced-order model in this simulation can be expressed as Gordeyev and Thomas (2013)

$$\dot{x}_1 = b_1 + L_{11}x_1 + Q_{141}x_1x_4 + Q_{111}x_1^2 + Q_{121}x_1x_2 + Q_{131}x_1x_3,$$

$$\dot{x}_2 = b_2 + \left[L_{22} + t_2\left(x_2^2 + x_3^2\right)\right]x_2 + L_{23}x_3 + Q_{121}x_1x_2,$$

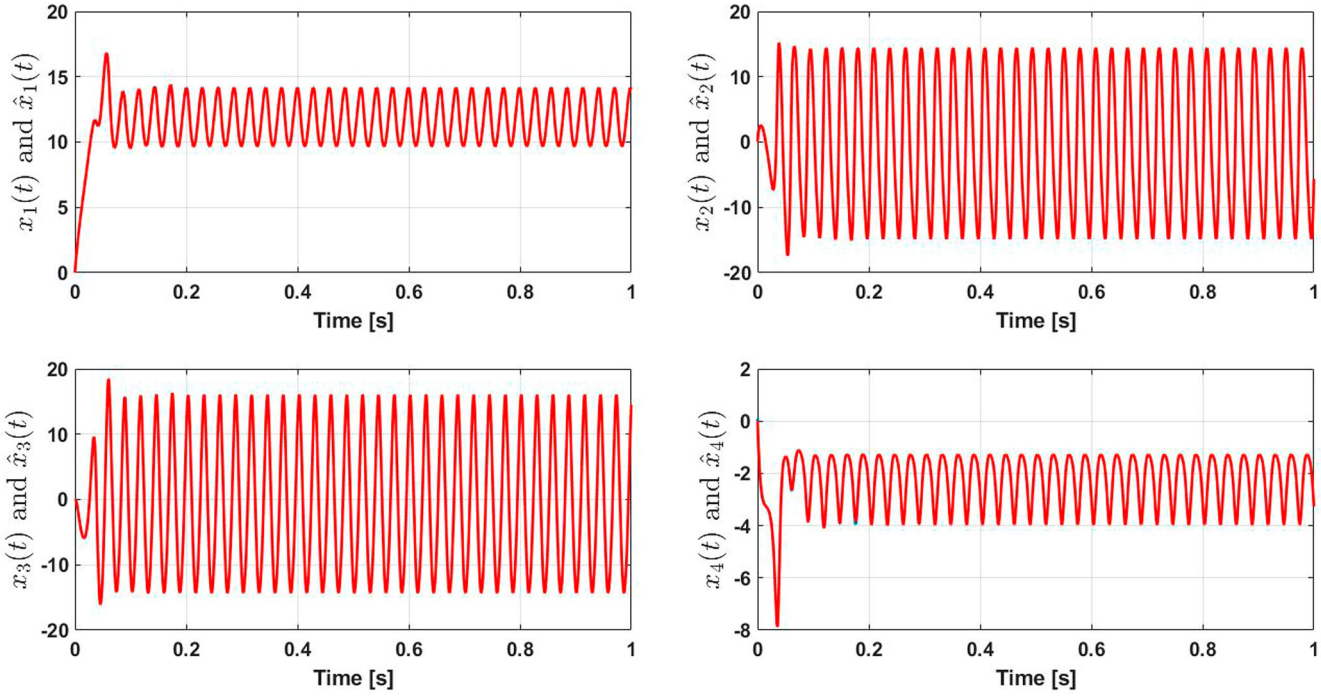

Figure 1. Time evolution of the states and the estimates using the observer in (19).

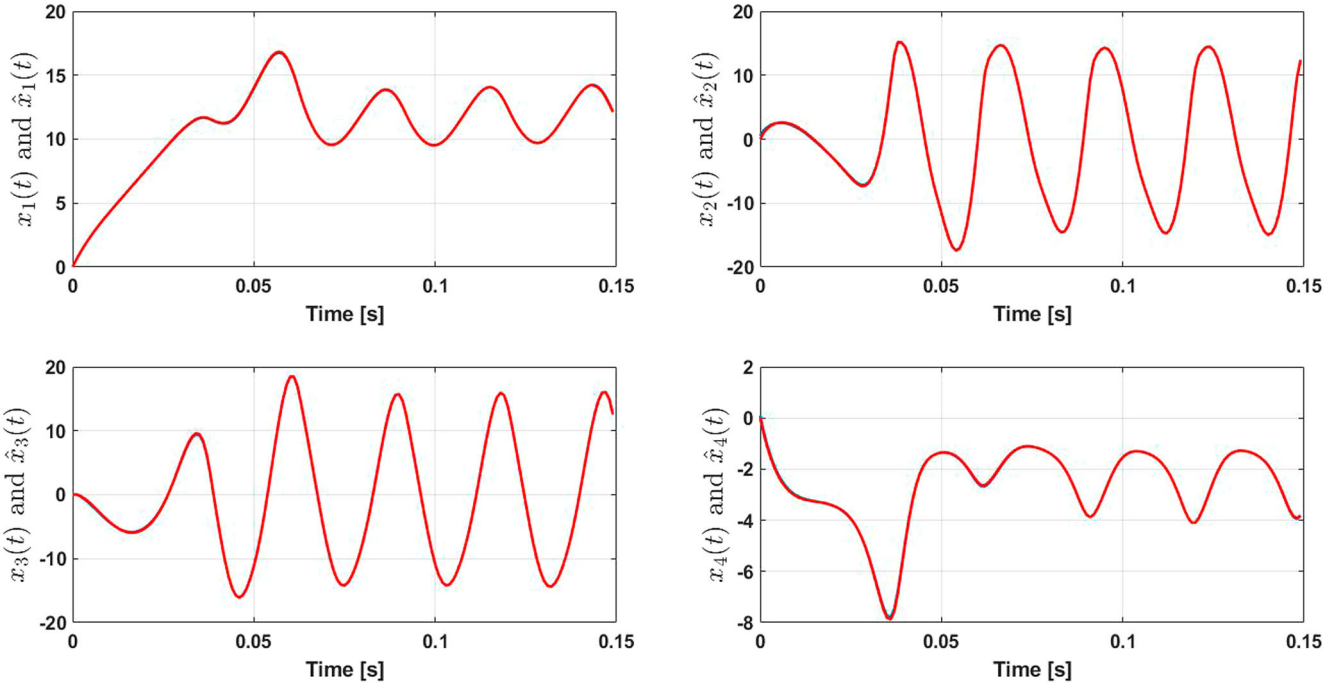

Figure 2. Zoomed plots showing the initial convergence phase of the states and the estimates using the observer in (19).

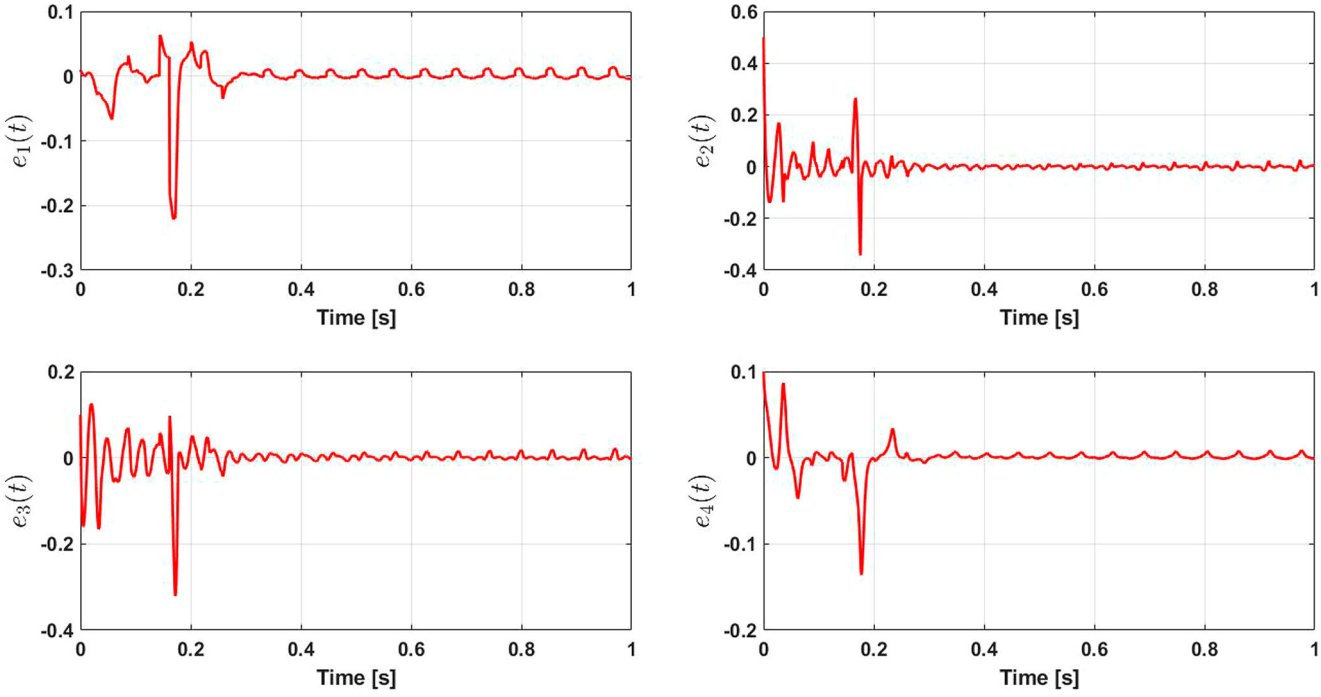

Figure 3. Time evolution of the error in each state over the entire simulation time.

$$\begin{aligned}\dot{x}_3 &= b_3 + L_{32}x_2 + \left[L_{33} + t_3\left(x_2^2 + x_3^2\right)\right]x_3 \\ &\quad + Q_{313}x_1x_3, + Q_{314}x_1x_4 \\ \dot{x}_4 &= b_4 + L_{41}x_1 + L_{44}x_4 + Q_{444}x_4^2 + Q_{414}x_1x_4 \\ &\quad + Q_{424}x_2x_4 + Q_{434}x_3x_4 \end{aligned} \tag{52}$$

with a measurement (i.e. output) equation given by

$$y = x_1 + x_2 + x_3 + x_4. \tag{53}$$

Thus, based on (52) and (53), the simulation plant model is in the form of (12) and (13), where $x : [0, \infty) \to \mathbb{R}^4$ and $y : \mathbb{R}^4 \to \mathbb{R}$. For completeness in defining the simulation plant model, the values of the constant parameters b_i, L_{ij}, Q_{ijk} for $i, j, k = 1, \ldots, 4$ are provided in Table 1.

The initial values for the states and estimates were selected as

$$\begin{aligned} x_1 &= 0.01, \quad x_2 = 0.5, \quad x_3 = 0.1, \quad x_4 = 0.1 \\ \hat{x}_1 &= 0, \quad \hat{x}_2 = 0, \quad \hat{x}_3 = 0, \quad \hat{x}_4 = 0 \end{aligned}$$

Figures 1, 2 and 3 show the observer performance for estimator gains selected as (see (19) and (20))

$$m_1 = 7, \quad m_2 = 7, \quad m_3 = 7, \quad m_4 = 2.$$

Figure 1 shows that the SMO reliably estimates the true states, even under the highly oscillatory state response. To clarify the results, Figure 2 shows the initial transient response of SMO system and Figure 3 shows the time evolution of the error. The results demonstrate the capability of the proposed SMO design to reliably estimate the unmeasurable state of the system.

7. Conclusion

A rigorous error system development and stability analysis are presented, which are based on a hierarchical SMO strategy containing multiple discontinuities. The hierarchical structure of the SMO is shown to achieve finite-time estimation of the complete state vector using a single scalar measurement, which could be a nonlinear function of the state in general. The challenge involved in analysing the convergence behaviour of the estimation error dynamic equations with discontinuous RHS is addressed through the use of differential inclusions in a Lyapunov-based framework. The result is a Lyapunov-based stability analysis that proves finite-time state estimation, while also incorporating a formal treatment of the multiple discontinuities inherent in the SMO design. Numerical simulation results are provided to demonstrate the capability of the SMO to estimate the full state of a fluid flow dynamic system using only a single available sensor measurement. Future work will address a rigorous analysis of the SMO as part of a closed-loop nonlinear control system under model uncertainty.

Disclosure statement

No potential conflict of interest was reported by the authors.

Funding

This work was supported by the National Science Foundation [grant number 1809790]; Directorate for Engineering [grant number 1809790].

ORCID

Krishna Bhavithavya Kidambi http://orcid.org/0000-0002-7266-3765

References

Brogliato, B., & Heemels, W. M. H. (2009). Observer design for Lur'e systems with multivalued mappings: A passivity approach. *IEEE Transactions on Automatic Control*, *54*(8), 1996–2001.

Chatterjee, A. (2000). An introduction to the proper orthogonal decomposition. *Current Science*, *78*(7), 808–817.

Clarke, F. (1983). *Optimization and nonsmooth analysis*. Reading, MA: Addison-Wesley.

Clarke, F. H., Ledyaev, Y. S., & Stern, R. J. (1998). Asymptotic stability and smooth Lyapunov functions. *Journal of Differential Equations*, *149*(1), 69–114.

Doris, A., Juloski, A. L., Mihajlovic, N., Heemels, W., van de Wouw, N., & Nijmeijer, H. (2008). Observer designs for experimental non-smooth and discontinuous systems. *IEEE Transactions on Control Systems Technology*, *16*(6), 1323–1332.

Drakunov, S. V (1992). Sliding-mode observers based on equivalent control method. In *Decision and Control, 1992., Proceedings of the 31st IEEE Conference on* (pp. 2368–2369).

Drakunov, S., & Utkin, V. (1992). Sliding mode control in dynamic systems. *International Journal of Control*, *55*(4), 1029–1037.

Filippov, A. F. (1988). *Differential equations with discontinuous right-hand sides*. Norwell, MA: Kluwer.

Filippov, A. F. (2013). *Differential equations with discontinuous righthand sides: Control systems* (Vol. 18). Netherlands: Springer.

Fischer, N., Hughes, D., Walters, P., Schwartz, E. M., & Dixon, W. E. (2014). Nonlinear rise-based control of an autonomous underwater vehicle. *IEEE Transactions on Robotics*, *30*(4), 845–852.

Fischer, N., Kamalapurkar, R., & Dixon, W. E. (2013). Lasalle-Yoshizawa corollaries for nonsmooth systems. *IEEE Transactions on Automatic Control*, *58*(9), 2333–2338.

Floquet, T., & Barbot, J.-P. (2006). State and unknown input estimation for linear discrete-time systems. *Automatica*, *42*(11), 1883–1889.

Floquet, T., & Barbot, J.-P. (2007). Super twisting algorithm-based step-by-step sliding mode observers for nonlinear systems with unknown inputs. *International Journal of Systems Science*, *38*(10), 803–815.

Fridman, L., Shtessel, Y., Edwards, C., & Yan, X.-G. (2008). Higher-order sliding-mode observer for state estimation and input reconstruction in nonlinear systems. *International Journal of Robust and Nonlinear Control: IFAC-Affiliated Journal*, *18*(4–5), 399–412.

Goebel, R., Sanfelice, R. G., & Teel, A. R. (2009). Hybrid dynamical systems. *IEEE Control Systems Magazine*, *29*(2), 28–93.

Gordeyev, S. V., & Thomas, F. O. (2013). A temporal proper decomposition (tpod) for closed-loop flow control. *Experiments in Fluids*, *54*(3), 1477.

Guo, Z., & Huang, L. (2009). Generalized Lyapunov method for discontinuous systems. *Nonlinear Analysis: Theory, Methods & Applications*, *71*(7–8), 3083–3092.

Holmes, P., Lumley, J. L., & Berkooz, G. (1996). *Turbulence, coherent structures, dynamical systems, and symmetry*. Cambridge: Cambridge University Press.

Kaplan, W. (1991). *Advanced calculus*. Reading, MA: Addison-Wesley.

Khalil, H. K. (1996). *Nonlinear systems*. Prentice-Hall, NJ, 2(5), 5–1.

Kidambi, K. B., MacKunis, W., Ramos-Pedroza, N., & Drakunov, S. V (2017). Active flow control under actuator uncertainty using a sliding mode estimation strategy. In *IEEE Conference on Control Technology and Applications (CCTA)* (pp. 7–12).

Kidambi, K. B., Ramos-Pedroza, N., MacKunis, W., & Drakunov, S. V. (2019). A closed-loop nonlinear control and sliding mode estimation strategy for fluid flow regulation. *International Journal of Robust and Nonlinear Control*, *29*(3), 779–792.

Kidambi, K. B., Ramos-Pedroza, N., MacKunis, W., & Drakunov, S. V (2016). Robust nonlinear estimation and control of fluid flow velocity fields. In *Decision and Control (CDC), 2016 IEEE 55th Conference on* (pp. 6727–6732).

Krasovskii, N. N. (1963). *Stability of motion*. Stanford, CA: Stanford University Press.

Levant, A. (2003). Higher-order sliding modes, differentiation and output-feedback control. *International Journal of Control*, *76*(9–10), 924–941.

Liu, K.-Z., Sun, X.-M., Liu, J., & Teel, A. R. (2016). Stability theorems for delay differential inclusions. *IEEE Transactions on Automatic Control*, *61*(10), 3215–3220.

MacKunis, W., Drakunov, S. V., Reyhanoglu, M., & Ukeiley, L (2011). Nonlinear estimation of fluid flow velocity fields. In *IEEE Conf. on Decision and Control and European Control Conference* (pp. 6931–6935).

Matusik, R., Nowakowski, A., Plaskacz, S., & Rogowski, A (2018). Finite-time stability for differential inclusions with applications to neural networks. arXiv preprint arXiv:1804.08440.

Nekvinda, A., & Zajíček, L. (1988). A simple proof of the Rademacher theorem. *Časopis pro pěstování matematiky*, *113*(4), 337–341.

Osorio, M., & Moreno, J. A (2006). Dissipative design of observers for multivalued nonlinear systems. In *Decision and Control, 2006 45th IEEE Conference on* (pp. 5400–5405).

Paden, B., & Sastry, S. (1987). A calculus for computing Filippov's differential inclusion with application to the variable structure control of robot manipulators. *IEEE Transactions on Circuits and Systems*, *34*(1), 73–82.

Sadikhov, T., & Haddad, W. M. (2015). A universal feedback controller for discontinuous dynamical systems using nonsmooth control Lyapunov functions. *Journal of Dynamic Systems, Measurement, and Control*, *137*(4), 041005.

Shevitz, D., & Paden, B. (1994). Lyapunov stability theory of nonsmooth systems. *IEEE Transactions on Automatic Control*, *39*(9), 1910–1914.

Shi, K., Tang, Y., Zhong, S., Yin, C., Huang, X., & Wang, W. (2018). Nonfragile asynchronous control for uncertain chaotic Lurie network systems with Bernoulli stochastic process. *International Journal of Robust and Nonlinear Control*, *28*(5), 1693–1714.

Shi, K., Wang, J., Zhong, S., Zhang, X., Liu, Y., & Cheng, J. (2019). New reliable nonuniform sampling control for uncertain chaotic neural networks under Markov switching topologies. *Applied Mathematics and Computation*, *347*, 169–193.

Shtessel, Y., Edwards, C., Fridman, L., & Levant, A. (2014). *Sliding mode control and observation*. Newyork: Springer.

Slotine, J. J. E., & Li, W. (1991). *Applied nonlinear control*. Englewood Cliff, NJ: Prentice Hall.

Tanwani, A., Brogliato, B., & Prieur, C. (2014). Stability and observer design for Lur'e systems with multivalued, nonmonotone, time-varying nonlinearities and state jumps. *SIAM Journal on Control and Optimization*, *52*(6), 3639–3672.

Teel, A. R., Nešić, D., Lee, T. -C., & Tan, Y. (2016). A refinement of Matrosov's theorem for differential inclusions. *Automatica*, *68*, 378–383.

Utkin, V. I. (2013). *Sliding Modes in Control and Optimization*. Berlin, Heidelberg: Springer-Verlag.

Utkin, V. I (1978). Sliding modes and their applications in variable structure systems. *Mir, Moscow*.

Vijayakumar, V. (2018). Approximate controllability results for analytic resolvent integro-differential inclusions in Hilbert spaces. *International Journal of Control*, *91*(1), 204–214.

Wang, J., Shi, K., Huang, Q., Zhong, S., & Zhang, D. (2018). Stochastic switched sampled-data control for synchronization of delayed chaotic neural networks with packet dropout. *Applied Mathematics and Computation*, *335*, 211–230.

Appendix

This appendix provides a detailed derivation of the time instants t_n for $i = 1, \ldots, n$, which are introduced in Equation (36) of Theorem 5.1.

The Lyapunov candidate function defined in Equation (37) is given as

$$V_i = \frac{1}{2} e_i^2 \Rightarrow |e_i| = \sqrt{2V_i}. \tag{A1}$$

By generalising the expression in (44), $\forall i = 1, 2, ..n$, which is given as

$$\dot{V}_i \leq -\kappa_i |e_i| \tag{A2}$$

$$\mathrm{d}V_i \leq \kappa_i |e_i| \mathrm{d}t, \tag{A3}$$

integrating on both sides, by using Equation (A1)

$$\int_{V_i(0)}^{V_i(t)} \frac{1}{\sqrt{2V_i}}\,\mathrm{d}V_i \leq \int_0^{t_i} \kappa_i\,\mathrm{d}t \tag{A4}$$

$$\frac{1}{\sqrt{2}}\left[2\sqrt{V_i(t)} - 2\sqrt{V_i(0)}\right] \leq -\kappa_i[t_i - 0] \tag{A5}$$

$$\sqrt{2V_i(t)} \leq \kappa_i t_i + \sqrt{2V_i(0)} \tag{A6}$$

$$|e_i(t)| \leq |e_i(0)| - \kappa_i t_i \tag{A7}$$

$$t_i = \frac{|e_i(0)|}{\kappa_i}, \quad \text{for } i = 1, \ldots, n. \tag{A8}$$